A Hub Dynamometer for Measurement of Wheel Forces in Off-Road Bicycling

D. S. De Lorenzo
Research Assistant.

M. L. Hull
Professor of Mechanical Engineering and Chair of Biomedical Engineering.

Department of Mechanical Engineering, University of California, Davis, Davis, CA 95616

A dynamometric hubset that measures the two ground contact force components acting on a bicycle wheel in the plane of the bicycle during off-road riding while either coasting or braking was designed, constructed, and evaluated. To maintain compatibility with standard mountain bike construction, the hubs use commercially available shells with modified, strain gage-equipped axles. The axle strain gages are sensitive to forces acting in the radial and tangential directions, while minimizing sensitivity to transverse forces, steering moments, and variations in the lateral location of the center of pressure. Static calibration and a subsequent accuracy check that computed differences between applied and apparent loads developed during coasting revealed root mean squared errors of 1 percent full-scale or less (full-scale load = 4500 N). The natural frequency of the rear hub with the wheel attached exceeded 350 Hz. These performance capabilities make the dynamometer useful for its intended purpose during coasting. To demonstrate this usefulness, sample ground contact forces are presented for a subject who coasted downhill over rough terrain. The dynamometric hubset can also be used to determine ground contact forces during braking providing that the brake reaction force components are known. However, compliance of the fork can lead to high cross-sensitivity and corresponding large (>5 percent FS) measurement errors at the front wheel.

Introduction

Designers of off-road bicycle frames and components face several challenges. One is the optimization of the suspension for minimum energy loss, maximum rider comfort, and maximum controllability. Another is balancing the requirement for light weight with the need for adequate structural reliability.

To meet these challenges, information regarding the loads to which the rider/bicycle system is subjected during off-road cycling is essential. Basically there are two possible approaches for providing this information. One is through dynamic system modeling and simulation (Wilczynski and Hull, 1994) and the other is by direct measurement. Because the results of simulations using dynamic system models must be experimentally verified, a system of dynamometers that could measure the loads input to the system is a necessity for either approach.

Previous work has focused on the development of dynamometers to measure forces between the rider and the bicycle, including dynamometric handlebars, pedals, and seatposts (e.g., Hoes et al., 1968; Hull and Davis, 1981; Bolourchi and Hull, 1985; Newmiller et al., 1988; Stone and Hull, 1993; Rowe et al., 1998) but no work known to the authors has developed a dynamometer to measure ground contact forces. Thus the objective of the project described in this paper was to design and evaluate dynamometers for measuring contact forces between both the front and rear wheels and the ground.

In considering the design criteria for such dynamometers, they must provide realistic measurement of loads when integrated into existing equipment and offer sufficient strength structurally to withstand the rigors of the off-road environment. Sufficient strength is important for reliable operation in an off-road environment that is characterized by high-magnitude inertial loads that develop while traveling over a rough surface (Wilczynski and Hull, 1994). To provide realistic measurements, the design both must allow the use of wheels built from standard components (i.e., hub shells, spokes, rims, and tires) and must mount to the frame and fork with minimal structural modification.

Another design requirement is that the dynamometer must accurately measure the two in-plane force components during off-road cycling situations likely to develop high-magnitude inertial loads. The ground reaction on a bicycle tire can be broken into its three force components, the radial Fz and tangential Fx components acting in the plane of the wheel and the transverse component Fy acting out of the plane of the wheel, and a moment component acting about the radial direction, Mz (see Fig. 1). The out-of-plane forces are anticipated to be small in relation to in-plane forces that develop as a consequence of high-magnitude inertial loads. Moments transmitted by the tires, for example from rider steering torque inputs, are measurable via handlebar-mounted instruments. Therefore, the dynamometer must measure the radial and tangential force components while offering low cross-sensitivity to the transverse force and to moments about the hub center. Also, because high-magnitude inertial loads are likely to be developed during downhill riding over rough terrain, the dynamometers must measure these two components while either coasting or braking but not necessarily during pedaling.

Design Description

To meet the criteria given above effectively, the dynamometers were fabricated by modifying existing commercially available hubs. The primary modification was replacing the original axles with specially designed axles equipped with strain gages judiciously located such that they could be connected into Wheatstone bridges where the bridge signals were sensitive to the loads of interest and insensitive to the extraneous (i.e., unmeasured) loads. Four strain gages were placed circumferentially at 90 deg intervals at two cross sections that were equidistant from the center of the axle as defined by the center of the bearings. Connecting the gages on opposite surfaces of the two cross sections into two full Wheatstone bridge circuits (Fig. 2)

Contributed by the Bioengineering Division for publication in the JOURNAL OF BIOMECHANICAL ENGINEERING. Manuscript received by the Bioengineering Division June 19, 1997; revised manuscript received October 8, 1998. Associate Technical Editor: A. G. Erdman.

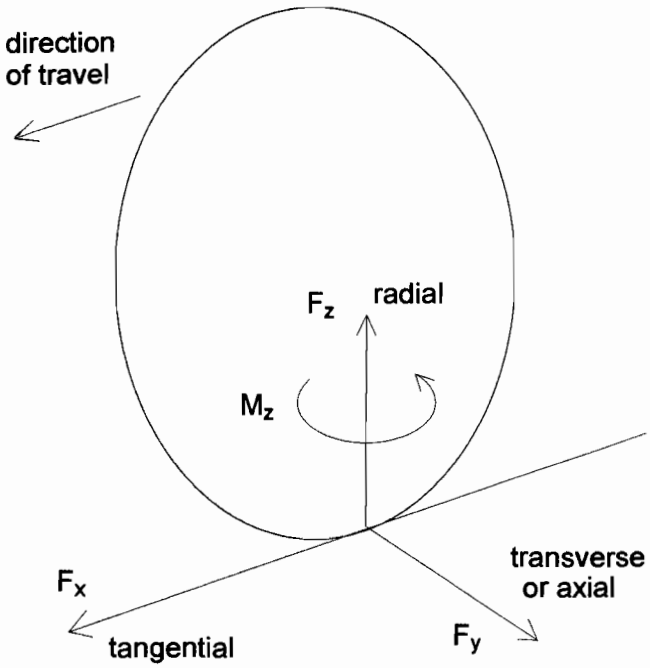

Fig. 1 Wheel schematic and ground contact reaction loads

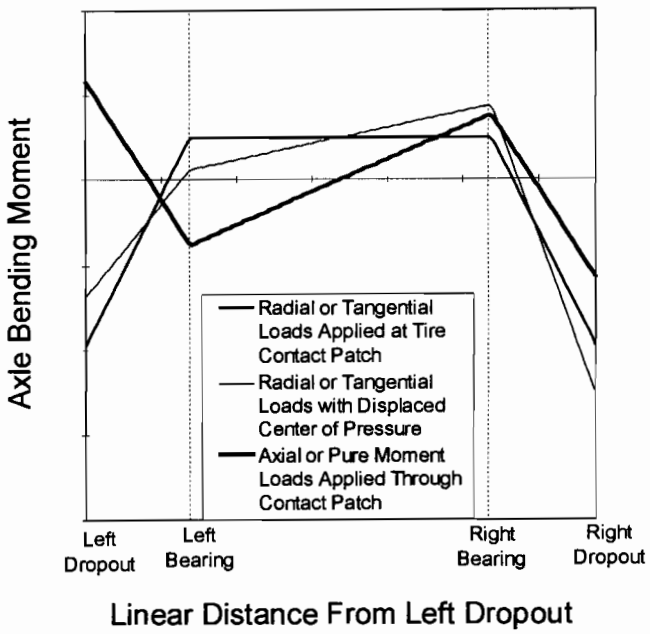

Fig. 3 Axle bending moment diagrams for three cases of loads applied through tire contact patch

gave outputs to each of the two desired loads developed during coasting; these bridge outputs were theoretically decoupled from one another.

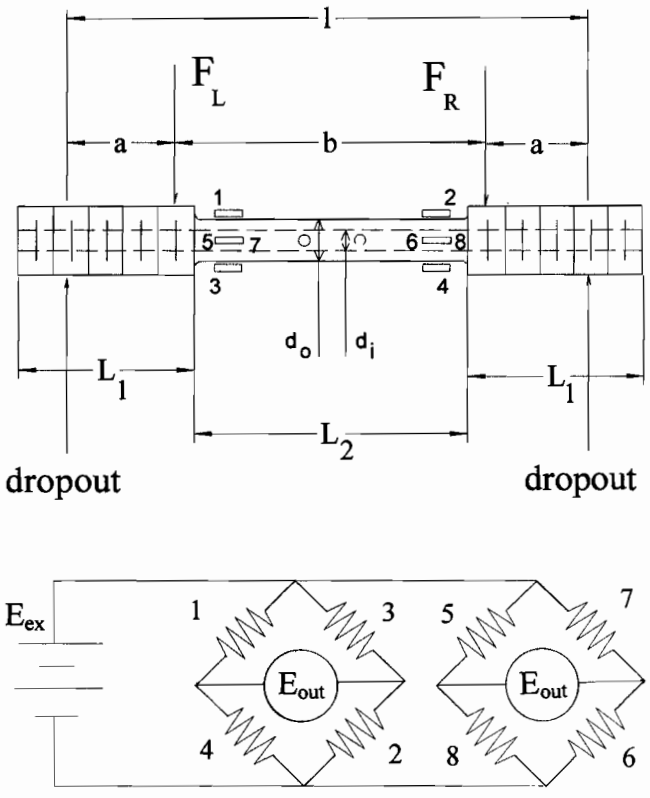

Fig. 2 Dynamometric axle drawing illustrating geometric parameters, reaction forces, and strain gage attachment and wiring diagram. In the drawing F_R and F_L are the right and left bearing reaction forces, respectively, caused by a radial force component F_z. The holes near the center of the axle are for routing the strain gage wires from the axle surface through the hollow inside diameter of the axle.

The arrangement and interconnection of the gages also gave bridge outputs that were insensitive to both the transverse force Fy and moment Mz. In the case of Fy applied at the contact point, this load creates an axial force along the axle and a pure moment between the bearing supports, whereas the moment Mz creates a pure moment only. Because the bending moment diagram is antisymmetric for these reaction moments (Fig. 3), the bridge outputs are insensitive to them from the traditional bridge output equation $E_{out} = (\epsilon_1 + \epsilon_2 - \epsilon_3 - \epsilon_4)\, GF\, E_{ex}/4$. In this equation, E_{ex} is the bridge excitation voltage, GF is the gage factor, the ϵ's are the strains, and E_{out} is the bridge output voltage. Also the axial force reaction was effectively negated because the normal stresses are all of the same sign.

To confirm that the bridge outputs were also insensitive to the point of load application of Fx and Fz (i.e., center of pressure not at the center of the tire), the bending moment in the axle was analyzed. In the region between the bearings, the bending moment as a function of the distance, x, along the axle from the left dropout, is given by:

$$M(x) = F_L\left\{\frac{(a+b)^2}{l^3}\,[x(4a+b) - al] - (x-a)\right\} + F_R\left\{\frac{a^2}{l^3}\,[x(4a+3b) - (a+b)l]\right\} \quad (1)$$

where F_L and F_R are the left and right bearing reactions, respectively, due to either Fx or Fz, l is the distance between dropouts, a is the distance from a dropout to its adjacent bearing (for a symmetric hub), and b is the distance between bearings (see Fig. 2). (Note: for notational convenience, the substitution $l = 2a + b$ has not been made in every case). If the point of load application is not centered between the bearings but instead has eccentricity e from the center, then bearing reactions F_L and F_R will differ in magnitude according to $F_L = F\,(\frac{1}{2} + e/b)$ and $F_R = F\,(\frac{1}{2} - e/b)$ where F is either Fx or Fz. Based on Eq. (1), the corresponding bending moment diagram for the axle is not symmetric along the length of the axle (Fig. 3). However, the sum of the moments developed at the strain gage locations is independent of the lateral location of the center of pressure (and is proportional to the sum of the applied radial and tangential

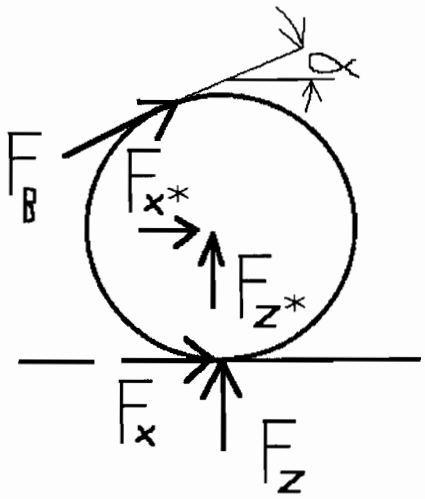

$$F_x = F_{x*} + F_B \cos\alpha$$

$$F_z = F_{z*} + F_B \sin\alpha$$

Fig. 4 Front wheel free-body diagram and equations for computing ground contact forces when the brake force is applied and measured and the hub loads are measured. F_x^* and F_z^* are the measured force components acting on the hub, F_B is the measured brake force component tangential to the rim, α is the angle that F_B makes with the ground, and F_X and F_Z are the computed ground contact force components.

loads). Accordingly because the total strain experienced by gages in the Wheatstone bridges is constant, the bridge outputs were independent of the center of pressure.

Although the measured hub forces directly indicate the ground contact force during coasting, this direct relation does not apply during braking because braking causes a reaction force at the hubs (Fig. 4). Thus, to determine the ground contact forces during braking, the brake force component tangential to the wheel rim was also measured. To measure this force, strain gages were applied to the post connecting the brake pad to the brake arms and connected in a Wheatstone bridge to measure shear in the post (Rowe et al., 1998). Front tire ground reaction forces could then be calculated in theory based on the equations given in Fig. 4.

Based on principles of static failure analysis, the axle dimensions (Table 1) and material were chosen to meet the conflicting requirements of high strength and high sensitivity. With a total force equal to five times the weight of a 90 kg (200 lb) rider and 18 kg (40 lb) experimental bicycle applied to either wheel, maximum stresses in the front and rear axle were 153 MPa and 261 MPa, respectively. Given the yield strength of the 17 − 4 stainless steel chosen as the material (1175 MPa), respective factors of safety were 7.7 and 4.5. With the modulus of elasticity

Table 1 Front and rear axle dimensions

Dimension	Front axle	Rear axle
a	16.0 mm	27.5 mm
b	70 mm	80 mm
l	102 mm	135 mm
d_o	7.62 mm	0.826 mm
d_i	0.445 mm	0.445 mm
L_1	35.6 mm	53.3 mm
L_2	61.0 mm	63.5 mm
Thread	M9 × 1	M10 × 1

Table 2 Front and rear hub calibratable sensitivity matrices [V/N] (normalized for gain and excitation voltage)

Front Hub

$$[V_x \quad V_z] = [F_x \quad F_z]\begin{bmatrix} -8.7369E-7 & 1.6722E-7 \\ 1.2484E-7 & 9.0736E-7 \end{bmatrix}$$

Rear Hub

$$[V_x \quad V_z] = [F_x \quad F_z]\begin{bmatrix} -1.6549E-6 & 8.7043E-8 \\ 5.1022E-9 & 1.6691E-6 \end{bmatrix}$$

of stainless steel equal to 190 GPa, the maximum strains at full-scale load were 805 $\mu\epsilon$ and 1375 $\mu\epsilon$, respectively. These factor of safety and strain values are for the center of pressure at the center of the tire. If the center of pressure is at the edge of the tire, then the stresses increase by 60 percent, causing a corresponding increase in the maximum strains and a reduction in the factors of safety.

After the axles were fabricated and the strain gages installed, the axles were assembled with the hubs. The strain gage wires were passed through the axles to the left, non-drive side, after which the axles were assembled into standard bicycle hubs: Shimano XT 32-spoke front and Specialized free-wheel-type 36-spoke rear. Since it was necessary to build each wheel with the rim centered between the bearing supports to gain the insensitivity of Wheatstone bridge outputs to variations in the center of pressure, spacers and a five-speed free wheel were used for the rear hub. When the hubs were eventually installed into the dropouts of the fork and rear triangle, the axles were accurately oriented (±1 deg) so that one plane of the strain gages corresponded to the plane of the ground surface. Finally, the wheels were installed in the dropouts using nuts and the strain gage wires were protected in epoxy-filled, cast metal elbows.

Calibration

Static calibration of the instrumented hubs was performed in a rigid test stand capable of applying forces and moments to the wheel rim using a system of weights and pulleys. Because the compliance within the bicycle frame, fork, and dropouts will affect the stresses imparted to the axles by applied loads, the wheels that contained the hubs were installed into an aluminum bicycle frame and suspension fork mounted within the test stand. In all cases, weights were increased incrementally until the maximum desired load was reached and then decreased incrementally. The same cycle was repeated in the negative direction, giving a complete loading cycle for each axle. The maximum force applied in the x and z directions was 667 N; for the y direction, a force of 178 N, causing a moment at the hub of 50 Nm, was applied. The x and z moments each received a maximum of 20 Nm. The My moment was not applied because this moment is produced from bearing friction and thus can be neglected. Linear regression was used to find the best-fit line relating the output voltages of each strain gauge circuit to the applied loading (Table 2).

The direct sensitivities and calibratable cross-sensitivities (i.e., cross-sensitivity to a measured load component) were highly linear (minimum R-square values of 0.999 and 0.972, respectively). The exception was the rear hub z-force cross-sensitivity (R-square value of 0.471). Being down by over two orders of magnitude from the direct z-force sensitivity, this low R-square value did not introduce appreciable error, and is possibly attributable to small ($\ll$1 deg) alignment errors. In any event, calibratable cross-sensitivities were accounted for in the calibration matrices (i.e., the inverse of the sensitivity matrices) to minimize the error.

As a result of the high linearity demonstrated by R-square values, nonlinearity and hysteresis errors were small. Relative

Table 3 Front and rear hub non-calibratable sensitivity matrices [V/N or V/Nm] (normalized for gain and excitation voltage)

Front Hub

$$[V_x \quad V_z] = [F_y \quad M_x \quad M_z] \begin{bmatrix} 9.9775E-8 & -1.8357E-7 \\ 8.9693E-8 & -4.0644E-7 \\ 8.6784E-7 & -2.2534E-7 \end{bmatrix}$$

Rear Hub

$$[V_x \quad V_z] = [F_y \quad M_x \quad M_z] \begin{bmatrix} 3.6614E-7 & -5.1300E-7 \\ 1.2326E-6 & -1.5270E-6 \\ 2.0931E-6 & -1.9460E-6 \end{bmatrix}$$

to the design load (i.e., five times body weight), in all cases the maximum nonlinearity measured as the maximum deviation between the calibration data and a linear fit to the loading data, taken in both the positive and negative directions, was less than 0.5 percent full scale (FS). Computed as the maximum deviation from zero output at zero load, the output hysteresis was less than 0.6 percent FS.

The cross-sensitivity to forces in the y direction was down by about a factor of 5 compared to in-plane forces (Table 3). In addition, since out-of-plane loads are typically small in relation to in-plane loads (Stone and Hull, 1993), this cross-sensitivity will not introduce appreciable error. For example, using the maximum calibration force value of 178 N, the maximum error was bounded by 1.2 percent FS for either hub for either of the two measured load components. The cross-sensitivity to moment loads was comparable, in units of V/Nm, to the direct dynamometer sensitivities, in units of V/N. Because the maximum moment loads are relatively small compared to the in-plane forces, the large cross-sensitivities to moment loads will not introduce significant errors. For example, using an experimental maximum steering torque of 33 Nm measured in a separate but unreported study in our laboratory, the largest response in the front hub was less than 1 percent FS for either the x or z directions.

By subjecting each hub to 10 combinations of the calibratable (i.e., measured) forces and noncalibratable (i.e., unmeasured) forces and torques, computing the apparent loads using the inverse of the calibration matrices contained in Table 2, and comparing these to the actual applied loads, an accuracy check was performed to determine measurement errors expected during coasting. With a maximum anticipated load of five times the weight of a 90 kg rider, the RMSE's for the front hub were 1.0 percent FS and 0.5 percent FS in the x and z directions, respectively; and the RMSE's for the rear hub were 0.6 percent FS and 1.0 percent FS in the x and z directions, respectively (Table 4).

The static calibration also included the determination of cross-sensitivity during front wheel braking where the components of the brake force create moments on the fork blade that are transmitted to the axle as a result of the fork blade compliance. Since the brake force was measured, this cross-sensitivity was calibratable. The front suspension fork from the test bicycle was attached to the test stand, and the front wheel mounted to

Table 4 Static and dynamic calibration results in the absence of braking

Calibration results	Linearity	Hysteresis	Accuracy (RMSE)	Natural frequency
Front X Force	0.24%	0.27%	1.02%	428 Hz
Front Z Force	0.28%	0.39%	0.46%	428 Hz
Rear X Force	0.36%	0.28%	0.55%	369 Hz
Rear Z Force	0.18%	0.42%	1.01%	369 Hz

Table 5 Front hub calibratable cross-sensitivity matrix to the applied tangential brake force component F_b, which is measured and the accompanying normal brake force component [V/N] (normalized for gain and excitation voltage)

$$[V_x \quad V_z] = F_b * [2.3302E-6 \quad -3.1804E-6]$$

it. Cables and pulleys were arranged such that a couple about the y axis was applied to simulate a deceleration ground reaction force. A couple was required since the sensitivity and cross-sensitivity to x axis forces at the ground contact were already known.

To equilibrate the applied couple, a series of loads were applied at the rim. Since the hub cross-sensitivity to brake forces was due to deformation of the fork structure during brake application, it was necessary to create both the normal and tangential components of the brake reaction force in applying the series of loads. Thus, the tangential brake force component just required to counteract the known couple was generated by squeezing the front brake lever until the load was (just) balanced. The voltage response of the front hub to this known tangential force was recorded for force values ranging from 0 N to 197 N. Note that since brake loads went from zero up to the applied wheel load during each load application (as the brake lever was squeezed), a hysteresis for this cross-sensitivity was not recorded.

The results indicated that the cross-sensitivities for both front hub outputs (Table 5) exceeded the direct sensitivities (Table 2). Although linear regression yielded R-squared values of 0.986 and 0.979 for Vx and Vz, respectively, the corresponding nonlinearities of 7.7 percent FS for Fx and 9.0 percent FS for Fz were large.

In addition to the static calibration, the natural frequency of each wheel assembly (i.e., the hub, spokes, rim, tire, and tube) in the radial mode (i.e., normal to the axle) was found by measuring the frequency during a free vibration test where the wheel was impacted while the axle was clamped in rigidly supported dropouts. For the front and rear wheels, natural frequencies were 428 Hz and 369 Hz, respectively.

Sample Loading Data

To demonstrate the utility of the front and rear hub dynamometers, data were collected from a full-suspension off-road bicycle (1995 FSR, Specialized Bicycle Components, Inc., Morgan Hill, CA). The test conditions involved a 77 kg rider, standing on the pedals with the crankarms nominally horizontal and the left foot forward, using the front brake for speed control, wearing 4.5 kg of test equipment, and coasting down a rocky fire road at 32 kph on a 14.5 kg bicycle. Front and rear suspension preload and air pressure were adjusted such that approximately one third of the available travel was consumed by the rider's static weight. The cartridge-type damper used in the front fork was set to its lightest position; the rear shock remained in its factory configuration. Data were logged by a purpose-built, portable data acquisition system allowing up to 32 channels of A/D input, with 12-bit converter resolution, and equipped with 256 K words of memory (Newmiller and Hull, 1990). The sampling rate was 200 samples/s on each of the channels recorded.

A 0.75 second segment of a 30 second, 300 meter trial was chosen for illustration (Fig. 5) since it includes a portion of time spent airborne, followed by a landing impact registering approximately 50 percent greater than the rider's weight. Several observations are noteworthy. First, the rider distributed a majority of his weight on the rear wheel of the bicycle, which is consistent with the findings of Rowe et al. (1998), who found that little weight was supported by the hands in the standing position. Next, different strategies are evident for the takeoff,

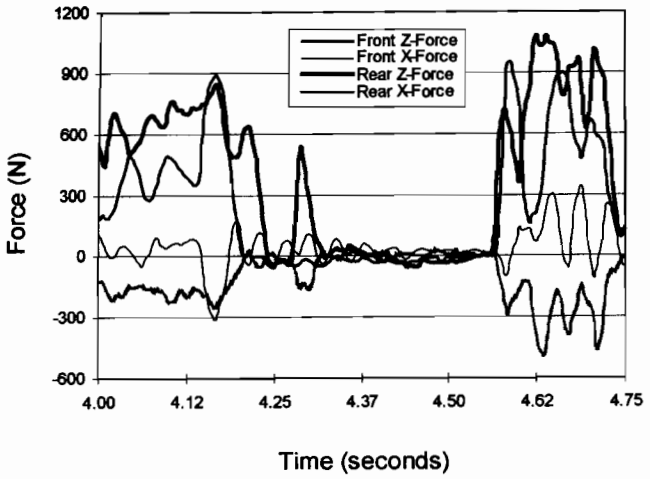

Fig. 5 Sample vertical and horizontal front and rear hub forces measured while coasting downhill at 9.0 m/s. The subject weighed approximately 750 N and was standing.

at 4.20 s, and landing, at 4.55 s. During the takeoff, the rider preweighted the front wheel, and then commenced the airborne maneuver with front wheel lift-off. The front wheel z force reached zero approximately 50 ms before the rear wheel; this corresponds to the time it took the bicycle to travel one-half wheelbase length at 32 kph. Landing was accomplished with both tires contacting the surface at the same instant, as can be seen by the simultaneous rise in the front and rear hub z forces. Finally, during the time in the air, small oscillations in the front wheel x force are apparent; this 26 Hz motion was possibly attributable to fore-aft vibration of the fork/front wheel assembly.

Discussion

The goal of the work reported in this paper was to design front and rear dynamometric hubs that would provide realistic and accurate measurements of the in-plane force components during off-road cycling. To assess the success of this design in reaching that goal, it is useful to evaluate the degree to which the design criteria were met.

One criterion was that the dynamometer provide a realistic picture of the loading. To give such a picture, the dynamometer had to be integrated into existing equipment with as little modification as possible, particularly to the wheels, since they were expected to influence the ground reaction loads strongly. One possible approach was to integrate the dynamometer into the dropouts. While this approach was feasible, it would have required substantial modifications to the fork and frame. Because such modifications would have been both time consuming and costly, the much simpler approach of integrating the dynamometer into the hub was taken. This approach required that only the axle be modified. Once installed into unmodified hub shells and properly positioned within the dropouts, the dynamometric hubs were indistinguishable from the normal hubs that they replaced.

To insure that the dynamometric hubs would withstand structurally the rigors of the off-road environment, the strength was an important consideration. Inasmuch as the use of the hubs was to be limited, only static strength and not fatigue strength was of interest. To determine static strength requirements, preliminary tests were conducted that used a force plate to measure the forces generated at the front and rear wheels during impact with the ground. These measurements indicated that impact loads of at least five times rider weight could be encountered on each wheel. Because this corresponds well with testing of the loads at rider contact points for simulated off-road riding (Wilczynski and Hull, 1994), five times rider weight was chosen as the design load. The maximum magnitude forces measured during experimental trials were 1550 N (350 lb) for the front hub and 4000 N (900 lb) for the rear hub, which supported the selection of a design load of five times rider weight.

The final criterion was that the dynamometric hubs measure the two in-plane force components accurately during both coasting and braking. The design presented meets this criterion for static loads developed during coasting. The direct sensitivity of the dynamometers to the radial and tangential forces was both linear and consistent. Although the cross-sensitivities to these forces were greater for the front than the rear dynamometer (Table 2), the cross sensitivities were calibratable and hence were accounted for in the data reduction. For the unmeasured load components, the error introduced by the noncalibratable sensitivities was minimal and had little effect on the measurement accuracy of the desired forces as evidenced by the low RMSE values from the accuracy check (Table 4).

To confirm the ability of the dynamometers to measure dynamic loads without inaccuracies due to resonance effects, the free vibration response was tested to determine the fundamental natural frequencies. The natural frequencies of 428 Hz and 369 Hz for the front and rear hubs, respectively, were more than 12 times the 30 Hz bandwidth of the hub loading measured during multiple experimental trials. Inasmuch as the fundamental frequency must be only about five times greater than the bandwidth to limit dynamic measurement errors to <5 percent of the corresponding static value (Doebelin, 1983), these natural frequencies are more than adequate.

One limitation is that the dynamometer can only reliably discriminate the radial and tangential components of the ground contact force so long as the angle that the radial force makes with the ground is close to 90 deg. If the wheel hits a log, for example, then the dynamometer is inherently incapable of separating the radial and tangential force components since the radial component will create large reactions in both the x and z directions at the hub. However, it should be recognized that any dynamometer would have this inherent limitation. Also, this does not limit the usefulness of the instrument because the force components input into the bicycle/rider system (i.e., hub forces) are still known.

A second limitation concerns the measurement accuracy during braking. One factor that affects the accuracy is the coefficient of friction between the rim and the brake pad. Before making the calculations indicated in Fig. 4, it was necessary to correct the axle bridge voltages for the cross-sensitivity due to the application of the brake forces. To make this correction, the cross-sensitivity was determined in the laboratory by applying both tangential and normal load components to the rim. Since the cross-sensitivity is governed by both load components and since only the tangential load component was measured in the field trials, applying this correction to the outputs measured in the field required the assumption that the coefficient of friction in the field was the same as that in the laboratory. This assumption was reasonably valid for the trials from which the sample data shown herein were taken since the trail was neither dusty nor muddy. If the coefficient of friction were to vary, then this assumption would not be valid so that it would be necessary to measure the normal brake force as well as the tangential brake force.

Even if both the normal brake force components are known accurately, however, the front hub loads are still subject to relatively large measurement errors compared to those in coasting owing to the high cross-sensitivity (Table 5) in conjunction with the large nonlinearity. Although an accuracy check was not performed under the application of brake forces, errors in individual load values as large as 8–9 percent FS could occur from the nonlinearity. Since the large cross-sensitivity is traced to the compliance in the fork, one possible approach for reducing this error would be to use a stiffer fork. Another possible approach would be to either reduce or eliminate the loads caus-

ing deformation of the fork. Torsional deformation could be minimized by redesigning the brake support structure so that the torsional moments created by the normal and tangential brake force components were equal in magnitude but opposite in direction, thus canceling on the fork blade.

For the rear dynamometer, not only do braking forces create reactions in the measured directions, but chain tension as a result of pedaling creates reactions as well. To avoid these reactions, the rear brake was disabled and the subjects coasted during the tests using the front brake only as necessary. Given the nature of the terrain over which the tests were conducted, the subjects easily modulated their speed with use of only the front brake. For more extreme conditions where the use of both brakes would be useful, the rear brake force could be measured similar to the front. In this case, the cross-sensitivity of the rear hub to rear brake forces may be substantially lower than that of the front hub if the rear wheel support structure is stiffer. A stiffer support structure for the rear wheel than the front wheel would be expected for most full suspension designs since the rear structure is typically triangular. For these designs, presumably the measurement errors would decrease accordingly.

Conclusion

This paper has presented instrumented front and rear bicycle hubs suitable for off-road use that accurately measure the radial and tangential tire contact forces independent of the other applied tire contact loads. Because these dynamometers are similar in function to commercially available hubs, they do not alter the loading conditions in any way. As demonstrated by the sample data, these dynamometers quantified the in-plane loads developed during off-road cycling while coasting. Quantification of these loads is useful for structural design studies, fatigue life prediction estimates, and the design of fatigue testing protocols. In addition, this quantification is useful for suspension design and optimization that affect rider comfort and control.

Acknowledgments

The authors express their gratitude to the following companies for their financial support: Cannondale, Dunlop Cycles, Easton, GT Bicycles, Mavic, Rockshox, Specialized Bicycle Components, Trek Bicycle Corporation, and True Temper Sports.

References

Bolourchi, F., and Hull, M. L., 1985, "Measurement of Rider Induced Loads During Simulated Bicycling," *International Journal of Sports Biomechanics,* 1(4):308–329.

Doebelin, E. O., 1983, *Measurement Systems,* 3rd ed., McGraw-Hill, San Francisco.

Hoes, M. J. A. J. M, Binkhorst, R. A., Smeekes-Kuyl, A. E. M. C., and Vissers, A. C. A., 1968, "Measurement of Forces Exerted on Pedal and Crank During Work on a Bicycle Ergometer at Different Loads," *Int. Z. angew. Physiol. einschl. Arbeitsphysiol.,* 26:33–42.

Hull, M. L., and Davis, R. R., 1981, "Measurement of Pedal Loading in Bicycling: I. Instrumentation," *Journal of Biomechanics,* 14(12):843–856.

Newmiller, J., Hull, M. L., and Zajac, F. E., 1988, "A Mechanically Decoupled Two Force Component Bicycle Pedal Dynamometer," *Journal of Biomechanics,* 21(5):375–386.

Newmiller, J., and Hull, M. L., 1990, "A 6800 Based Portable Data Acquisition Module With Advanced Performance Capabilities," *International Journal of Sports Biomechanics,* 6(4):404–414.

Rowe, T., Hull, M. L., and Wang, E. L., 1998, "A Pedal Dynamometer for Off-Road Bicycling," ASME JOURNAL OF BIOMECHANICAL ENGINEERING, 120(1):160–164.

Stone, C., and Hull, M. L., 1993, "Rider/Bicycle Interaction Loads During Standing Treadmill Cycling," *Journal of Applied Biomechanics,* 9(3):202–218.

Wilczynski, H., and Hull, M. L., 1994, "A Dynamic System Model for Estimating Surface-Induced Frame Loads During Off-Road Cycling," ASME *Journal of Mechanical Design,* 116(3):816–822.